AD NUMBER
AD810470
NEW LIMITATION CHANGE
TO Approved for public release, distribution unlimited
FROM Distribution authorized to U.S. Gov't. agencies and their contractors; Critical Technology; 13 JAN 1967. Other requests shall be referred to Naval Ordnance Labatory, White Oak, Silver Spring, MD.
AUTHORITY
NOL ltr, 15 Nov 1971

NUMERICAL HYDRODYNAMIC CALCULATIONS
OF THE FLOW OF THE DETONATION PRODUCTS
FROM A POINT-INITIATED EXPLOSIVE
CYLINDER

13 JANUARY 1967

NOL

UNITED STATES NAVAL ORDNANCE LABORATORY, WHITE OAK, MARYLAND

NUMERICAL HYDRODYNAMIC CALCULATIONS OF THE FLOW OF THE
DETONATION PRODUCTS FROM A POINT-INITIATED EXPLOSIVE CYLINDER

By

D. Piacesi, Jr.

ABSTRACT: With the use of the NOL two-dimensional hydrodynamics
computer program (CYCLONE), a detailed numerical analysis is made
of the flow in the product-gas of a detonating cylinder of pentolite
(50/50 PETN/TNT) explosive. The explosive cylinder is initiated at
a point on the central charge axis at one end-face. The detonation
front is assumed to be spherical. This is consistent with experimen-
tally determined wave shapes. The calculations are carried out to
the point where the detonation front is at 1.71-charge-diameters from
the point of initiation. The results of the calculations show that
the flow in the "detonation head" (region bounded by the detonation
front, and the lateral and rear rarefaction waves) is entirely
spherical. Moreover, this spherical flow is exactly that which is
described by the similarity solution of G. I. Taylor for a spherical
detonation wave.

EXPLOSION DYNAMICS DIVISION
EXPLOSIONS RESEARCH DEPARTMENT
U. S. NAVAL ORDNANCE LABORATORY
WHITE OAK, MARYLAND
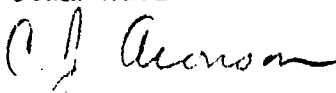
NOLTR 66-150   13 January 1967

NUMERICAL HYDRODYNAMIC CALCULATIONS OF THE FLOW OF THE
DETONATION PRODUCTS FROM A POINT-INITIATED EXPLOSIVE CYLINDER

This report discusses the results of numerical hydrodynamic

calculations on the flow in the product-gas resulting from the

detonation of a cylinder of explosive. This report will be of

interest to scientists who are dealing with experiments involving

point-initiated explosive cylinders, and to engineers concerned

with conventional explosive weapons design. This work was carried

out under NAVORD Task ORD-033-221/092-1/F008-08-11 Problem 004 -

Explosion Hydrodynamic Calculations.

                              E. F. SCHREITER
                              Captain, USN
                              Commander

                              C. J. ARONSON
                              By direction

                              ii

CONTENTS

ILLUSTRATIONS

I. INTRODUCTION

Let us examine the flow produced by the detonation of an unconfined right circular cylinder of high explosive, where the initiation is at a point on the central axis at one end-face (refer to Fig. 1). As the detonation progresses from the point of initiation, the gaseous explosion products expand out through the end-face. Consequently, a rarefaction wave travels into the gas behind the detonation front. When the detonation reaches the side of the cylinder, a shock is transmitted into the surrounding medium and a lateral rarefaction wave is reflected into the explosion products. Subsequently, the head of the lateral rarefaction wave impinges on the central charge axis and annihilates the rear rarefaction wave. The region bounded by the head of the lateral rarefaction and the detonation front is sometimes referred to as the "detonation head".[1]*

While considerable attention has been given to the detonation head, there does not appear to be in the literature any attempt to calculate the actual flow in the detonation head region. With the use of the Naval Ordnance Laboratory's two-dimensional hydrodynamics computer program, CYCLONE[2], a detailed numerical analysis of this transient compressible flow problem can be carried out. The results of calculations for a two-inch diameter cylinder of pentolite (50/50 PETN/TNT) explosive are presented in Sec. V of this report; The calculations were performed on an IBM-7090 computer.

* References are on Page 15.

II. THE PHYSICAL MODEL

We make the physical assumptions about the detonation that
(1) the chemical reaction zone is infinitely thin (i. e., the solid
explosive is instantaneously converted to gaseous products as the
shock-detonation front passes over it), (2) the Chapman-Jouguet (CJ)
conditions[3] hold at the detonation front, (3) the detonation propagates
in all directions from the point of initiation with the CJ detonation
velocity,* (4) the explosive is surrounded by a vacuum, and (5)
"edge" effects are negligible. Here, the term "edge" effects refers
to the radical change in the curvature of the detonation front near
the cylindrical surface of the charge. This effect is produced by
the influence of the lateral rarefaction wave on the chemical reaction
zone.

In solid high explosives, the width of the chemical reaction zone
is of the order of several millimeters and therefore assumption (1)
does not impose a too unreal restriction on the physical model.
Assumption (1) does, however, eliminate any effect of the lateral
rarefaction wave on the chemical reaction zone at the sides of the
cylinder. Hence, assumption (5) results as a natural consequence of
(1). In the experiments by Cook, et al.[1], the edge effect did not
exceed 2 mm in any case. Assumption (2) is introduced into the
calculations via the equation of state of the detonation-product gas
(see Sec. IV).

---

* The CJ detonation velocity is defined as $D = V_1 [(p_2 - p_1)/(V_1 - V_2)]^{\frac{1}{2}}$,
where p_1, V_1 (p = pressure, V = specific volume) is the initial state
of the solid unreacted explosive and p_2, V_2 is the point of tangency
of the Rayleigh line from P_1, V_1 to the reactive Hugoniot of the product
gas. This is the theoretical maximum steady-state velocity which the
detonation can achieve. See Ref. (3).

The shape of the detonation front directly affects the flow in the region behind the wave front. Assumption (3) imposes the requirement that the wave front coincide with the surface of an expanding sphere, whose radius of curvature is equal to the product of the CJ detonation velocity (D_{CJ}) and the time (t) elapsed after initiation. Cook, et al.,[1] and Jaffe and Clairmont[4], show experimentally that in point-initiated cylinders of "ideal" explosives* the detonation front is indeed initially spherical, and that the radius of curvature of the front is $D_{CJ}t$. However, there is a fundamental difference between the two sets of data. In the work by Cook, et al., the radius of curvature of the detonation front approaches a constant value by the time the wave has propagated a distance of less than four charge diameters from the point of initiation. From this point on, the detonation front propagates in a "steady state" condition. In the experimental work by Jaffe and Clairmont with two-inch diameter tetryl cylinders, the radius of curvature of the detonation front increases geometrically (radius = $D_{CJ}t$) at a distance of four charge diameters from the point of initiation with no indication of reaching a steady state. In the computer calculations which are described in this report, the mathematical model of the detonation is consistent with both sets of data, since the calculations were only carried out until the detonation front is at 1.71 charge diameters from the point of initiation. There is, however, an obvious extrapolation of the calculations which can be made in the light of the Jaffe-Clairmont experimental results. This is done in Sec. VI.

* We define an "ideal" explosive as one in which the detonation propagates at the theoretical maximum steady-state velocity (i.e., the CJ detonation velocity).

III. THE HYDRODYNAMIC EQUATIONS AND THE MATHEMATICAL MODEL

We can write the hydrodynamic equations for transient, isentropic, axially symmetric flow in Lagrangian form as follows: Denote the Lagrangian coordinates by k, l, the Eulerian coordinates by R, Z, the velocity components by u, v, the density by ρ, the specific volume by $V = (1/\rho)$, the internal energy by E, the pressure by p, and the time by t. Then the equations are

(continuity)
$$\frac{\rho_0}{\rho} = \frac{RA}{R_0 A_0} \quad , \tag{1}$$

where
$$A = \frac{\partial(R,Z)}{\partial(k,l)} \quad , \tag{2}$$

(momentum)
$$\frac{d^2 R}{dt^2} = \frac{-R}{\rho_0 R_0 A_0} \left[\frac{\partial p}{\partial k} \frac{\partial Z}{\partial l} - \frac{\partial p}{\partial l} \frac{\partial Z}{\partial k} \right] \quad , \tag{3}$$

$$\frac{d^2 Z}{dt^2} = \frac{-R}{\rho_0 R_0 A_0} \left[\frac{\partial p}{\partial l} \frac{\partial R}{\partial k} - \frac{\partial p}{\partial k} \frac{\partial R}{\partial l} \right] \quad , \tag{4}$$

$$u = \frac{dR}{dt} = \int \frac{d^2 R}{dt^2} dt \;, \quad v = \frac{dZ}{dt} = \int \frac{d^2 Z}{dt^2} dt \;,$$

$$R = \int \frac{dR}{dt} dt \;, \quad Z = \int \frac{dZ}{dt} dt \;,$$

(energy)
$$\frac{\partial E}{\partial t} = -p \frac{\partial V}{\partial t} \tag{5}$$

where the subscript zero refers to the initial state of the material. The equation of state for each material is assumed given in the form p = p(E,V).

The von Neumann-Richtmyer finite difference method, [1] which handles shocks automatically, is used for the numerical integration of the hydrodynamic equations. In this scheme, an artificial

4

dissipative term is introduced into the conservation of energy and momentum equations. This term causes shocks to have a finite thickness and makes the flow variables change abruptly but continuously through the region of the shock. In addition, the correct entropy change is effected across the shock. In CYCLONE, the artificial dissipative term is defined as

$$ q = \frac{b\,A}{V\,V_o^2}\left(\frac{\partial V}{\partial t}\right)^2 \tag{6} $$

where the variables A, V, and t are defined above and b is the shock-width constant, which can be adjusted to give the desired sharpness to the shock. The pressure, p, in equations (3), (4), and (5) is then replaced by $P = (p+q)$. The finite difference analogues of the hydrodynamic equations which are actually used in the numerical integration, can be found in Ref. 2.

Let us now briefly examine the mathematical model that is used in the finite difference method. As a result of the cylindrical symmetry, the three-dimensional flow can be represented by the flow in any R, Z ($R \geq 0$, θ = const) half plane (Fig. 2). Lagrangian coordinate (k,l) lines, imbedded in the material, divide the material into zones. Initially, the mass of each zone is calculated. This mass remains constant throughout the computations, thus assuring conservation of mass. There is then assigned to each mesh point (intersection of a k and an l line) a mass equal to one-fourth of the mass in the four surrounding zones. The velocity components of each

mass point and the pressure, internal energy, and density of each zone
are given as initial conditions.

At each computation cycle, the program calculates consecutively
for each zone ρ from the continuity equation, E and p from the
simultaneous solution of the energy equation and the equation of state,
and q from the formula given in eq. (6). At this point, a time step
for the integration is determined from stability conditions.[6] The
accelerations of each of the mass points are next determined by the
momentum equations. From the accelerations and the time step, the
new velocity components and positions of the mass points are then
obtained. The calculations are advanced in finite increments of time
by repeating the above steps at every integration cycle. The material
flow is thus determined by the motion of the mass points.

A programmed detonation scheme is used to instantaneously
convert the solid high explosive to gaseous explosion products. Since
we assume the detonation propagates with the constant CJ velocity
from the point of initiation, we therefore can calculate the position
of the detonation surface at each computation cycle. For each zone
containing solid explosive, a test is made to see if the detonation
front has arrived at the zone (corner nearest the point of initiation).
If it has arrived, the chemical energy of the solid explosive which
is contained in the zone is added to the internal energy of that zone*.
For this and subsequent time cycles, this zone uses the equation of
state for the gaseous explosion products. If the detonation has not

---

* In the reported calculations (Sec. V), the chemical energy was
actually added in discrete amounts of 1/3 the total chemical energy
in the zone as the detonation front passed over each 1/3 section of
the diagonal of the zone. By allowing the energy adjustment to take
place over several computation cycles, the typical oscillations found
in numerical calculations of this type were greatly reduced.

yet arrived, the equation of state of the solid unreacted explosive
is used.

IV. EQUATIONS OF STATE

In compressible fluid flow calculations, it is necessary to
have an equation of state for each material. The equations of state
which are used for the solid unreacted explosive and the detonation
product gases are discussed in this section.

When making numerical hydrodynamic calculations, it is often
a satisfactory approximation, at least for solids, to use the
shock Hugoniot (the locus of possible states which are attainable from
some initial state by a single shock transition) as an equation of
state. The equation of state for the solid unreacted Pentolite
explosive is taken as

$$p = 0.1282 \mu + 1.193 \mu^3, \tag{7}$$

where p is the pressure (megabars), $\mu = \rho/\rho_o - 1$, and ρ is the
density (g/cm^3). The subscript zero refers to the initial state.
Equation (7) may not closely represent the shock Hugoniot for
unreacted pentolite. It is probably more representative of the
shock Hugoniot for unreacted Composition B explosive (see, for
example, Ref. (7)). However, almost any reasonable form for the
equation of state is adequate for our calculations since the
detonation is programmed as a function of time and does not depend
on the state of the solid explosive. The form of the equation of
state for the solid explosive has essentially no effect on the flow
in the detonation-product gases.

The equation of state of the pentolite detonation-product gas is assumed to be given in the form[8]

$$p = (A\rho + B\rho^2) E + C\rho^3 \tag{8}$$

where A, B, and C are constants and p, E, and ρ are the thermodynamic variables described above. The value A = 0.35 is obtained by defining $A = (\gamma - 1)$, where γ is the average ideal gas specific heat ratios (c_p/c_v) of the detonation products. Equation (8) thus approaches the polytropic gas equation for small ρ. The constants B = 0.1243 and C = 0.01279 were chosen so that eq. (8) would reproduce the particular CJ detonation conditions and the CJ isentrope obtained by thermochemical calculations.*

The CJ detonation conditions for pentolite ($\rho_o = 1.65$) gotten with the thermochemical calculations are pressure $p_{CJ} = 0.2452$ megabars, density $\rho_{CJ} = 2.210$ g/cm³, sound speed $c_{CJ} = 0.5714$ cm/µsec, and detonation velocity D = 0.7655 cm/µsec. The value of the CJ specific internal energy $E_{CJ} = 0.0775$ megabar-cm³/g is obtained by calculating the area under the CJ isentrope from the CJ pressure to zero pressure. The chemical energy E_o which is used in the computer calculations is obtained from the Hugoniot relation

$$E_{CJ} - E_o = (P_{CJ} + P_o) (V_o - V_{CJ})/2. \tag{9}$$

This gives $E_o = 0.0587$ megabar-cm³/g. E_o is the energy which is added to the specific internal energy of a zone as the detonation front reaches the zone (see Sec. III).

---

* The thermochemical calculations were carried out by H. Hurwitz, using the RUBY computer program[9] which contains the Cowan-Fickett version of the Becker-Kistiakowsky-Wilson equation of state[10]. The modified RDX parameters of Mader[11] were used in the calculations.

V. RESULTS OF CALCULATIONS

The results of the calculations on the flow produced by the detonation of a two-inch cylinder of pentolite explosive are summarized in Figs. 3-12. Figures 3-10 and 12 were processed directly from the computer calculations (excluding the labels and dashed-in rarefaction fronts) on a Stromberg-Carlson SC-4020 Microfilm Recorder.

The cross section (parallel to the central axis) of the detonating cylinder is shown in Figs. 3-6 for different instants of time after initiation. Initiation of the detonation is at t=0. The Lagrangian computation grid is plotted on the cross section. The initial grid (Fig. 3) consists of approximately 4000 mesh points. Additional grid is generated as the detonation progresses down the cylinder. At t = 11.3841 microseconds the computation grid has 9000 mesh points (the top half of the grid shown in Fig. 6). The initial zone size of the solid explosive is 0.0508 x 0.05 cm. Individual zones in the solid explosive and the compressed explosion products cannot be clearly distinguished in the figures because of the inadequate resolution of the scale which was chosen for the plots. In Figs. 4-6, however, the zone configuration is discernible in the region where the gas has undergone some expansion. At 2.9753 microseconds after initiation (Fig. 4), the detonation has not yet reached the side of the cylinder. The detonation-product gas expands only out the end-face of the cylinder. After the detonation reaches the side of the cylinder (Fig. 5) the gas expands radially as well. The cross section at t = 11.3841 microseconds is shown in Fig. 6. The

Lagrangian grid line which was originally the end-face surface of the

solid explosive was dropped from the calculations at t = 9.9171 micro-

seconds and therefore does not appear in Fig. 6.

The pressure distribution in the product gas at specific times

after initiation is illustrated in Figs. 7-10. Here, the positions

of the isobars in the cross section of the detonation are shown.

The leftmost isobar is the 10 kilobar line. On each consecutive

isobar to the right, the pressure increases by 10 kilobars. The

detonation front is at the CJ pressure of 245 kilobars. The head

of the rear and lateral rarefaction waves are shown by dashed lines.

The head of the lateral rarefaction wave can be located on each isobar

($\geq$ 60 kb) at the point where the isobar departs from being circular.

On the central axis, the head of the rear rarefaction wave moves with

the 55 kb isobar. In Fig. 7, only the rear rarefaction wave exists.

In Figs. 8 and 9, both rarefactions can be seen. The head of the

lateral rarefaction impinges on the central axis at t = 11.3841 micro-

seconds (Fig. 10), thereby annihilating the rear rarefaction wave.

At subsequent times, the head of the rear rarefaction wave does not

appear.

It should be noticed that the flow is entirely spherical in

the region (detonation head) bounded by the heads of the rear and

lateral rarefaction waves and the detonation surface. Moreover, this

spherical flow is exactly that which is described by the similarity

solution of G. I. Taylor for a spherical detonation[12] (Hereafter

referred to as the spherical Taylor wave). In Fig. 11, the pressure

and particle velocity profiles along the central axis in the CYCLONE

calculations (t = 7.6359 microseconds) are compared to the pressure

and particle velocity distribution in a spherical Taylor wave.*

The two sets of data are shown to be in exact agreement in the region

where the Taylor wave particle velocity is greater than zero. The

departure of the two data in the Taylor wave region of zero particle

velocity is due to the two different boundary conditions at the

initiatior point. In the Taylor similarity solution the detonation

is spherical and the geometry imposes the boundary condition that

the gas at the point of initiation remain fixed. In the CYCLONE

calculations the detonation is hemispherical and the gas at the

point of initiation on the central axis is allowed to expand freely.

The expansion of the gas along the axis causes a rarefaction wave

to follow the detonation front. This rear rarefaction wave exists only

until it is annihilated by the lateral rarefaction wave impinging on

the central axis. Previous to this time, the penetration of the

rear rarefaction wave, along the axis, is known since the position of

the head of this wave must correspond with the "sonic point" (point of

zero particle velocity) in the Taylor wave. We see from Fig. 11 that

this is so.

---

* This Taylor wave was numerically generated with the use of
W. A. Walker's computer routines[13]. The equation of state for
the detonation products given in Sec. IV was used in the Taylor
wave calculations.

The effect of the von Neumann-Richtmyer finite difference method on the flow variables at the shock front is demonstrated in Fig. 11. The pressure and particle velocity profiles are "rounded" at the shock front and a small "tail" precedes the actual position of the shock front. This typical characteristic of the numerical method produces an inherent "edge" effect in the calculations. The "tail" causes the unreacted explosive at the cylindrical surface to expand before it is "detonated" by the computer program. Therefore the lateral rarefaction wave proceeds into the cylinder about 0.3 microseconds sooner than it would if the shock-detonation front were infinitely thin.

The specific volume (or density, since $\rho = 1/V$) distribution in the cross section of the detonating cylinder at t=11.3841 microseconds is shown in Fig. 12. The isochore furthest from the detonation front is V=1.50 cm^3/g. The specific volume decreases by 0.05 cm^3/g on each consecutive isochore closer to the detonation front. At the detonation front, the specific volume is $V=1/\rho_{CJ}=1/2.210=0.4525$ cm^3/g. The specific volume distribution in the detonation head region is identical to the specific volume distribution in a spherical Taylor wave.

VI. DISCUSSION

The results of the calculations (Sec. V) are, of course, only valid for that part of the detonation where our physical and mathematical model of the detonation is consistent with the experimental data. More specifically, it is valid over that region where the shape of the detonation front can be represented by an expanding sphere of radius $D_{CJ}t$. From the extensive experimental data of Cook,

et al[1]., this is shown to be for a charge length of 3.5 charge diameters for pentolite, in particular, and for charge lengths of 1 to 4 charge diameters for solid explosives, in general. Since the calculations were carried out to where the detonation front was 1.71 charge diameters from the point of initiation, we are well within the limitations of our model.

In addition to the specific numerical results obtained, more general conclusions can be made. We have shown that the flow immediately behind the detonation front in the region unaffected by the rear and lateral rarefaction wave, is, identically, the Taylor similarity flow for a spherical detonation. Since the characteristic of similarity flows is that the flow variables depend only on their relative position in the flow, we are able to determine the flow in this region for later times. That is, at least to the point where the radius of curvature of the detonation front is equal to 3.5 charge diameters which is the upper limit of our detonation model according to Cook's data. From the rather limited experimental data of Jaffe and Clairmont[4], the indication is that our model of the detonation may hold over a much greater distance. Therefore, perhaps, the Taylor similarity solution may be validly extended to charge lengths greater than 3.5 charge diameters.

It should be pointed out that although one can obtain the flow in the detonation head region for later times because it is a similarity flow, one cannot, however, determine the shape of this region by extrapolating the calculated results. The shape of the detonation head has to be determined by calculating the motion of the lateral rarefaction front into the spherical Taylor wave flow of the detonation head.

13

VII. ACKNOWLEDGEMENTS

VIII. REFERENCES

1. M. A. Cook, et al., J. Appl. Phys., $\underline{27}$, 269 (1956).

2. T. Orlow, D. Piacesi, and H. M. Sternberg, Naval Ordnance Laboratory Report NOLTR 7265, (September 1960).

3. Ia. B. Zeldovich and A. S. Kompaneets, Theory of Detonation, (Academic Press, New York and London, 1960).

4. I. Jaffe and A. R. Clairmont, Naval Ordnance Laboratory Report NOLTR 65-33, (June 1965).

5. J. Von Neumann and R. D. Richtmyer, J. Appl. Phys., $\underline{21}$, 232 (1950).

6. J. W. Enig, J. Math. and Phys., Vol XI, No. 1, (April 1961).

7. N. L. Coleburn and T. P. Liddiard, Jr., J. Chem. Phys., $\underline{44}$ 1929, (1966).

8. H. M. Sternberg and D. Piacesi, Phys. Fluids, $\underline{9}$, 1307, (1966).

9. H. B. Levine and R. E. Sharples, University of California, Lawrence Radiation Laboratory Report UCRL-6815, (March 1962).

10. R. D. Cowan and W. Fickett, J. Chem. Phys., $\underline{24}$, 932 (1956).

11. C. L. Mader, Los Alamos Scientific Laboratory Report LA-2900, (July 1963).

12. G. I. Taylor, Proc. Roy. Soc., A, $\underline{200}$, 235 (1950).

13. W. A. Walker and H. M. Sternberg, presented at Fourth Symposium on Detonation, (Oct 12-15, 1965), to be published in the proceedings (1967).

(1-a) CYLINDER OF HIGH EXPLOSIVE. INITIATION TAKES PLACE AT POINT ON CENTRAL AXIS AT ONE END FACE.

(1-b) CROSS SECTION OF THE EXPLOSIVE CYLINDER BEFORE THE DETONATION FRONT REACHES THE SIDE OF THE CYLINDER.

(1-c) CROSS SECTION OF THE EXPLOSIVE CYLINDER SHORTLY AFTER THE DETONATION FRONT REACHES THE SIDE OF THE CYLINDER.

(1-d) CROSS SECTION OF THE DETONATING CYLINDER AFTER A CONSIDERABLE LENGTH OF TIME FOLLOWING INITIATION. THE LATERAL RAREFACTION HAS ANNIHILATED THE REAR RAREFACTION.

FIG. 1 A QUALITATIVE DESCRIPTION OF THE FLOW IN A POINT-INITIATED CYLINDER OF EXPLOSIVE
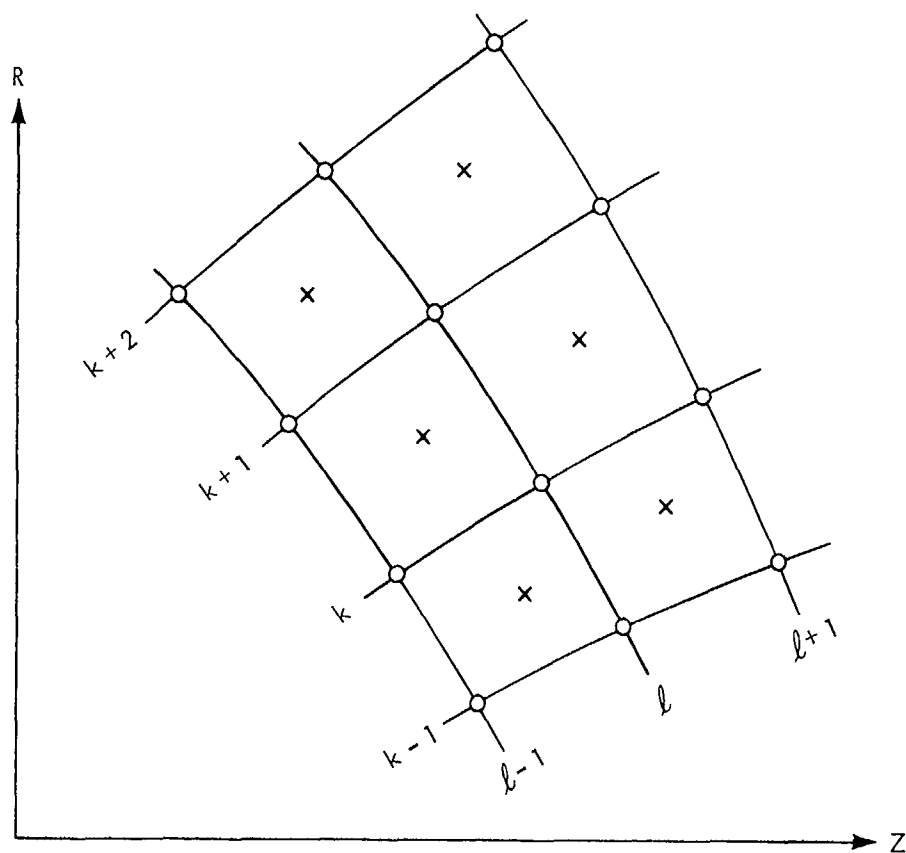
FIG. 2   A GENERAL LAGRANGIAN COMPUTATION GRID. MASS POINTS
ARE LOCATED AT THE INTERSECTION OF THE k, ℓ LINES.
POSITIONS AND VELOCITIES ARE ASSOCIATED WITH EACH
MASS POINT. PRESSURE, SPECIFIC VOLUME, INTERNAL ENERGY,
AND AN ARTIFICIAL VISCOSITY ARE LOCATED AT THE CENTER
(X's) OF THE QUADRILATERALS ("ZONES").
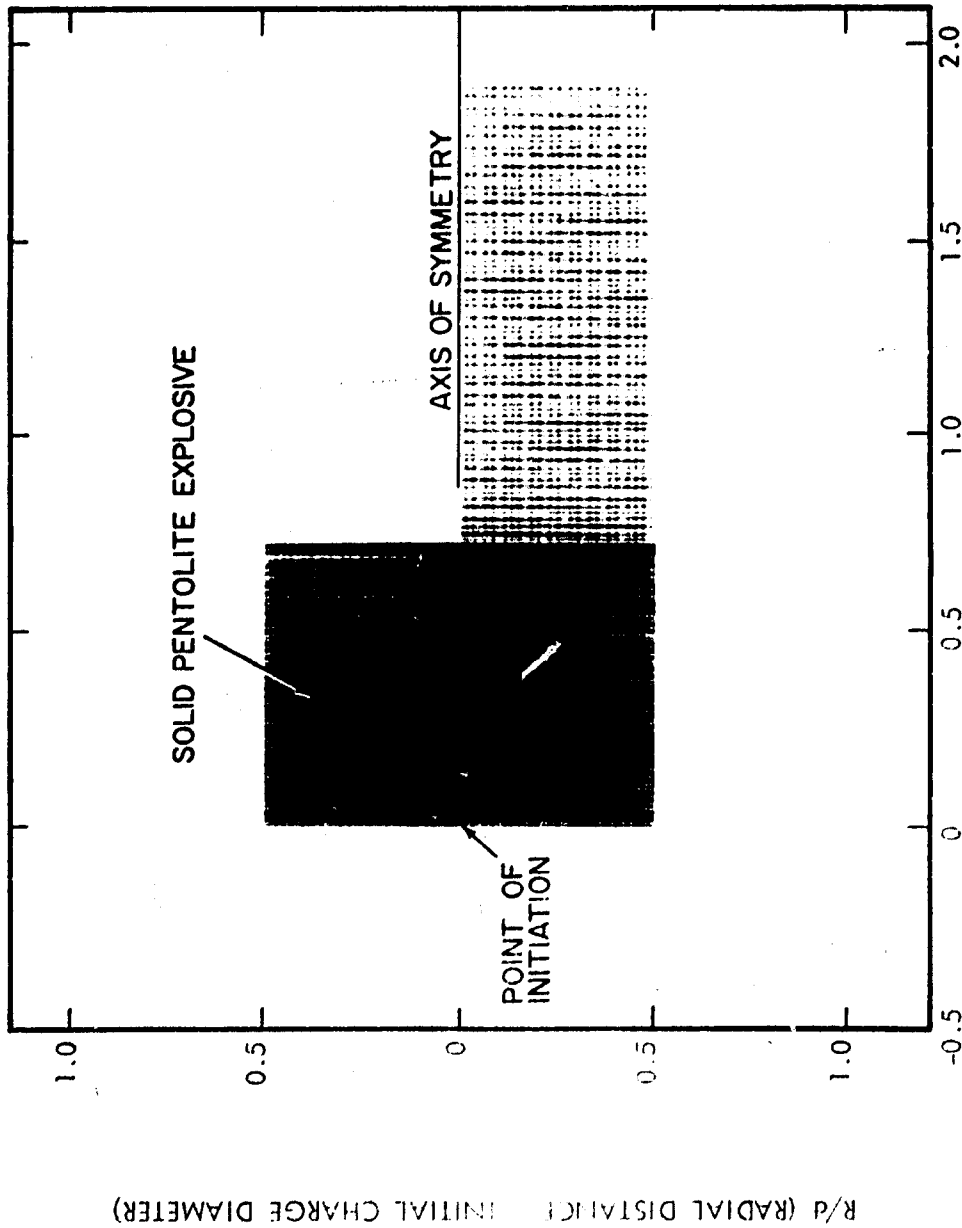
FIG. 3 Cross section of a two inch diameter cylinder of pentolite. The initial Lagrangian computation grid is shown on the cross section. The computations are made with the half of the grid which is above the axis of symmetry. The bottom half of the grid is plotted as the mirror image of the top half. The point of initiation is at $(R/d, Z/d) = (0,0)$.
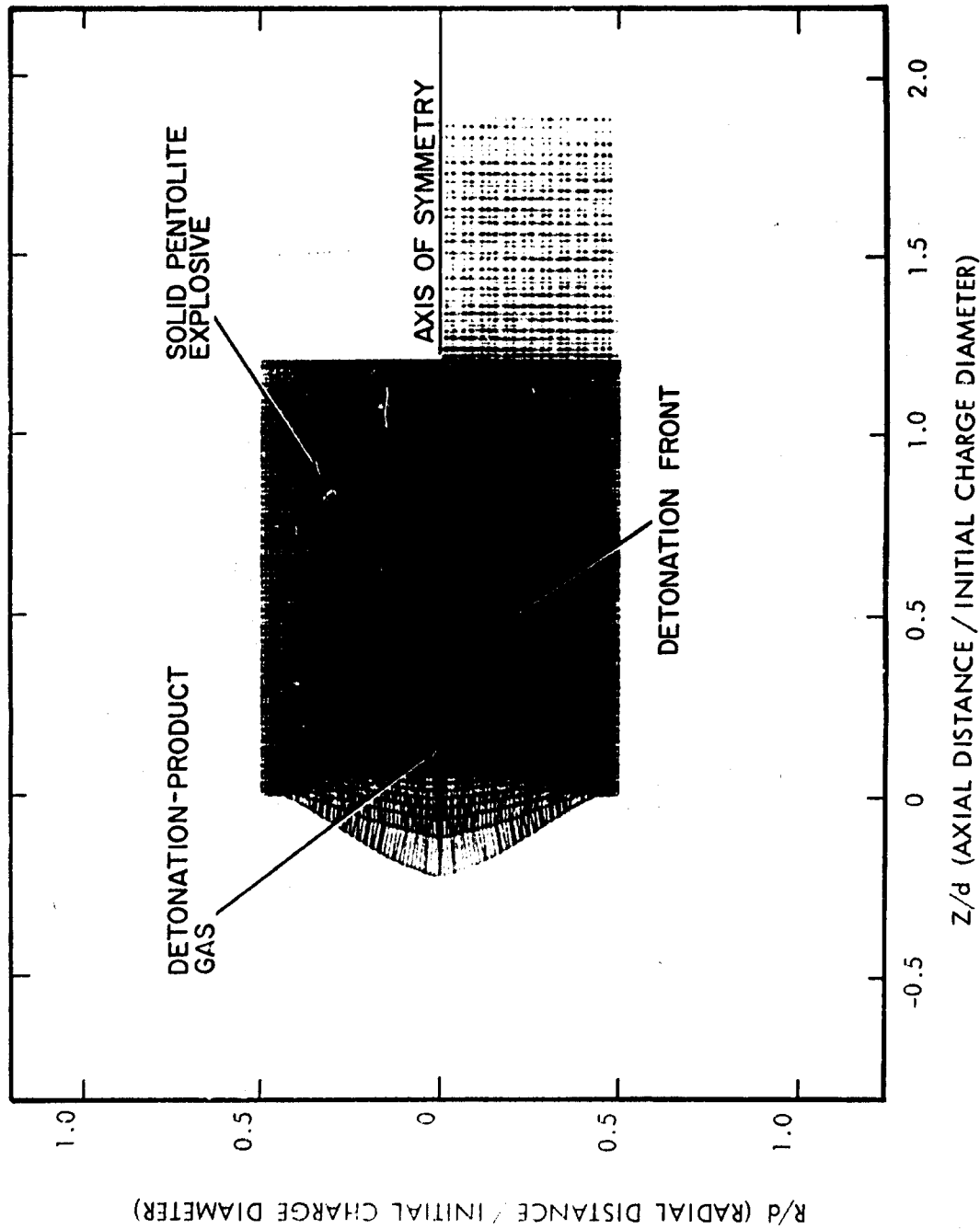
FIG. 4 Cross section of the detonating cylinder at 2.9753 μ seconds after initiation. The detonation front has not yet reached the side of the cylinder. Point of initiation is at (R/d, Z/d = (0,0).
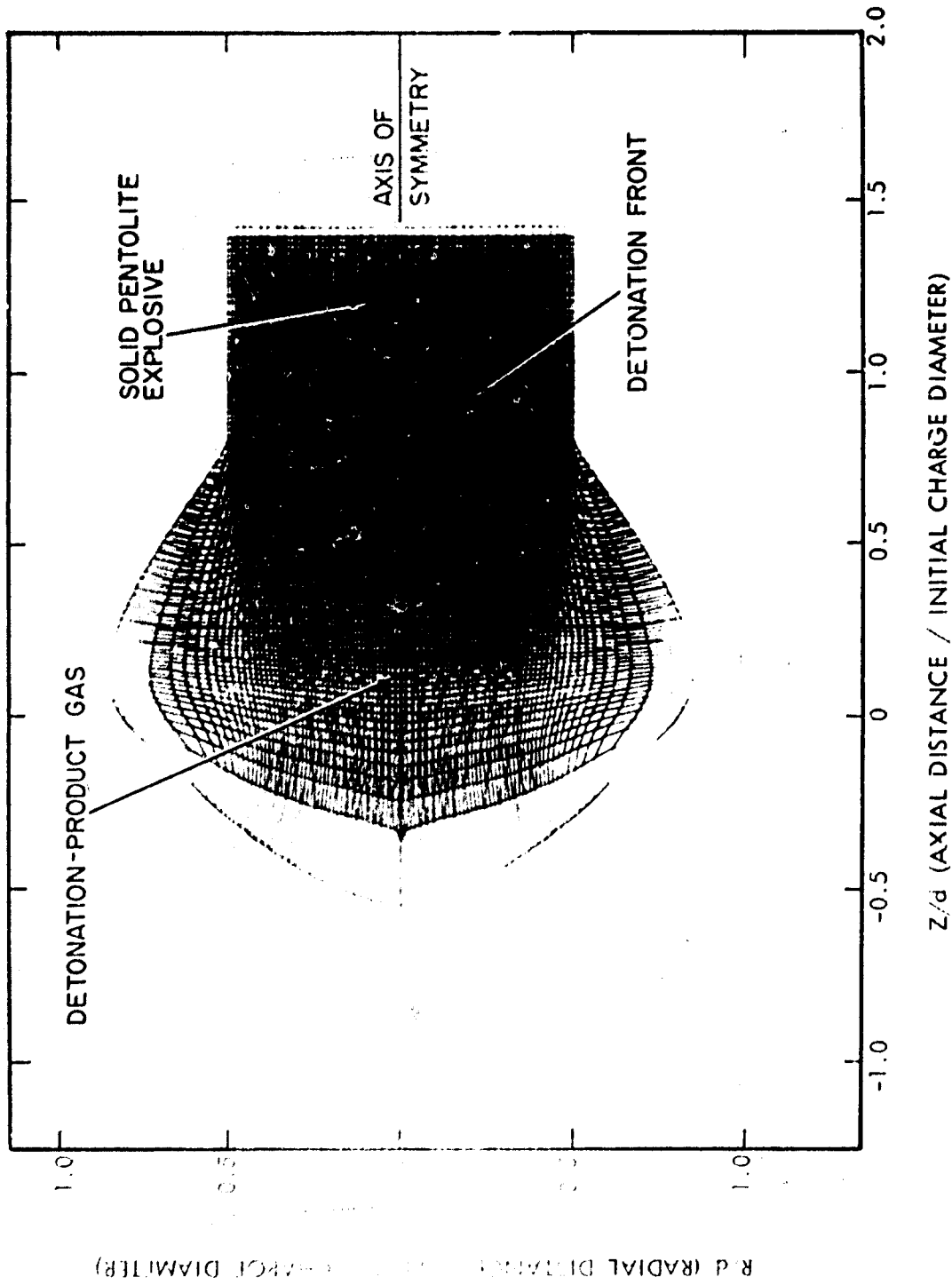
FIG. 5 Cross section of the detonating cylinder at 6.249 μseconds after initiation. The detonation front has reached the side of the cylinder and the detonation-product gas expands radially. Point of initiation is at (R/d, Z/d) = (0,0).
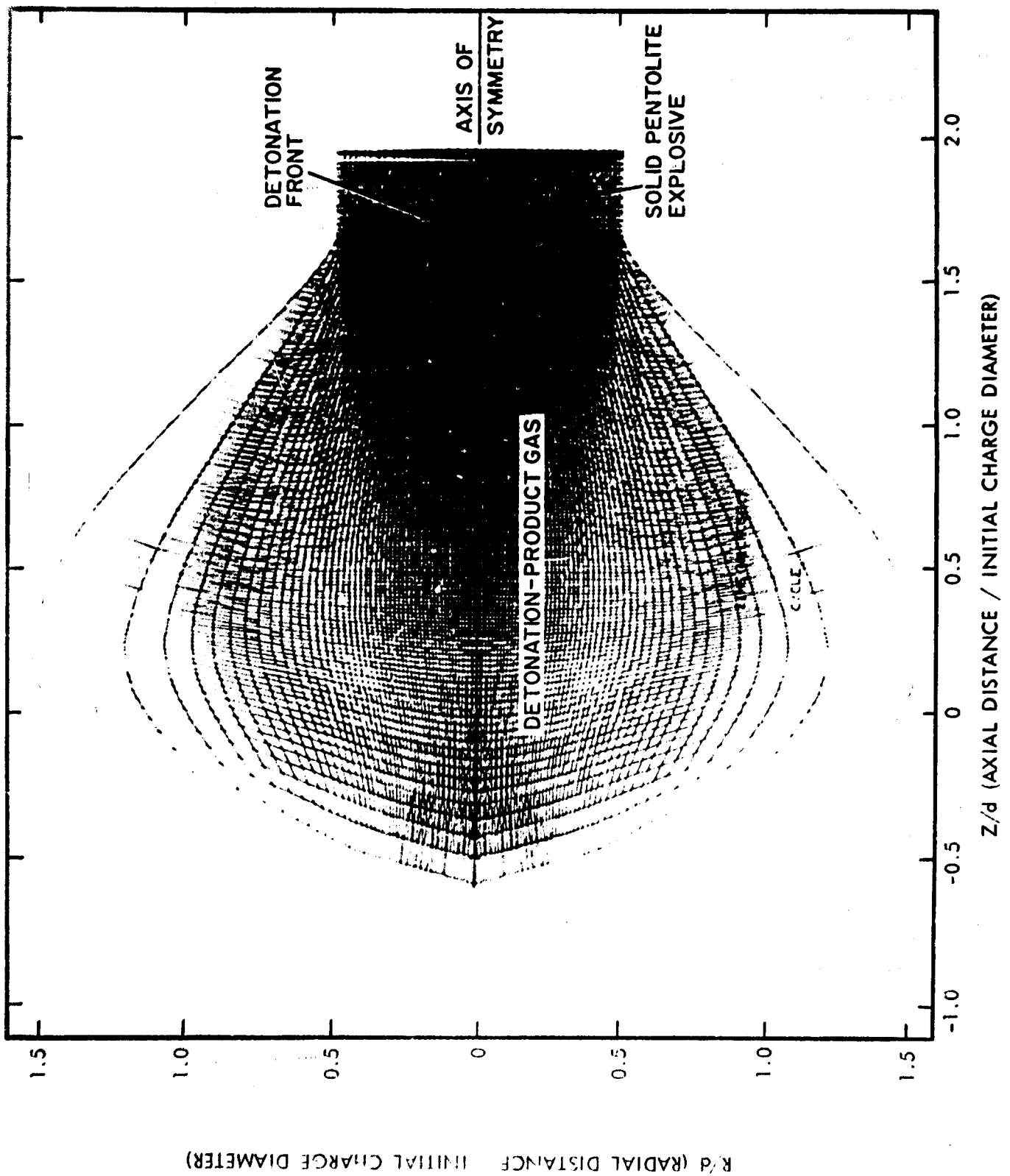
FIG. 5 Cross section of the detonating cylinder at 11.3841 μ seconds after initiation. Point of initiation is at $(R/d, Z/d) = (0,0)$.
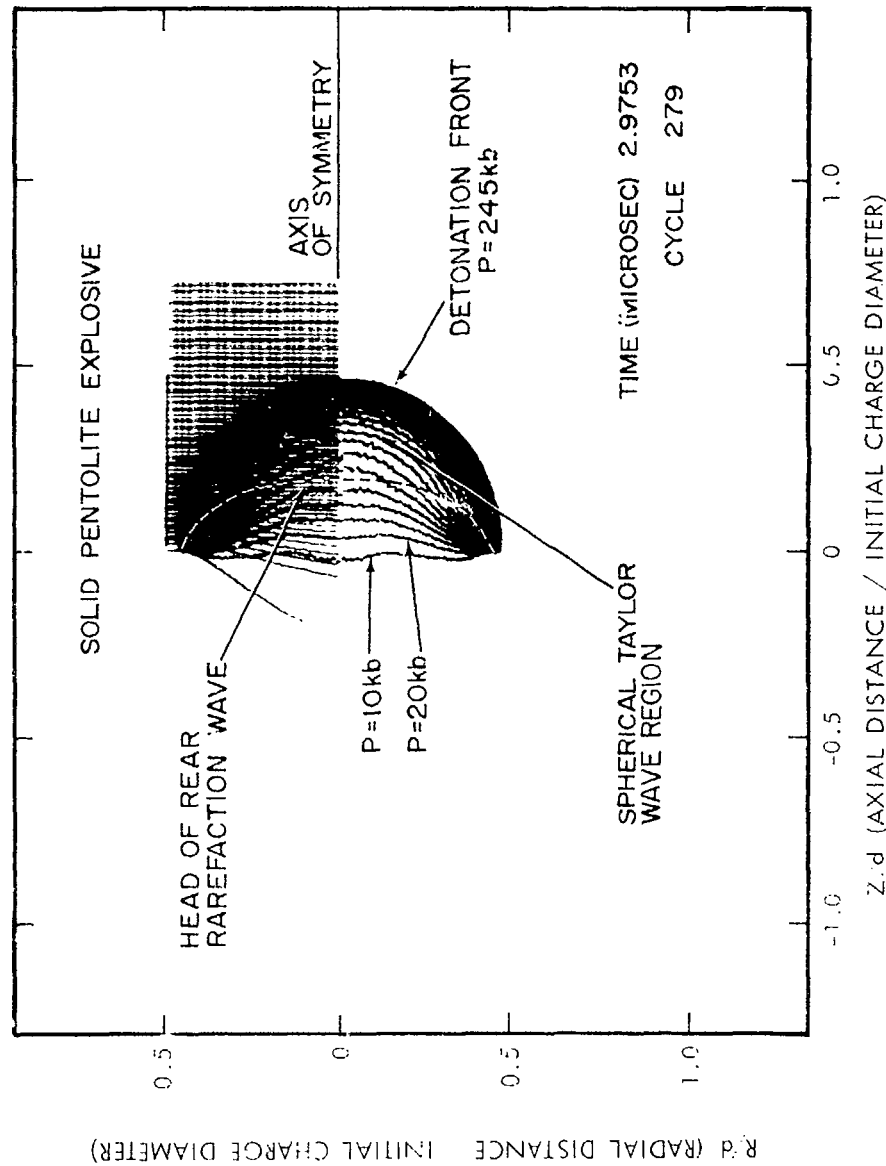
FIG. 7 The pressure distribution in the form of isobars is shown in the cross section of the detonating cylinder at 2.9753 μ seconds after initiation. There is a difference of 10 kilobars between adjacent isobar lines (actually a set of discrete points) with the leftmost isobar = 10kb and the pressure at the detonation front = 245kb. Point of initiation is at (R/d, Z/d) = 0,0.
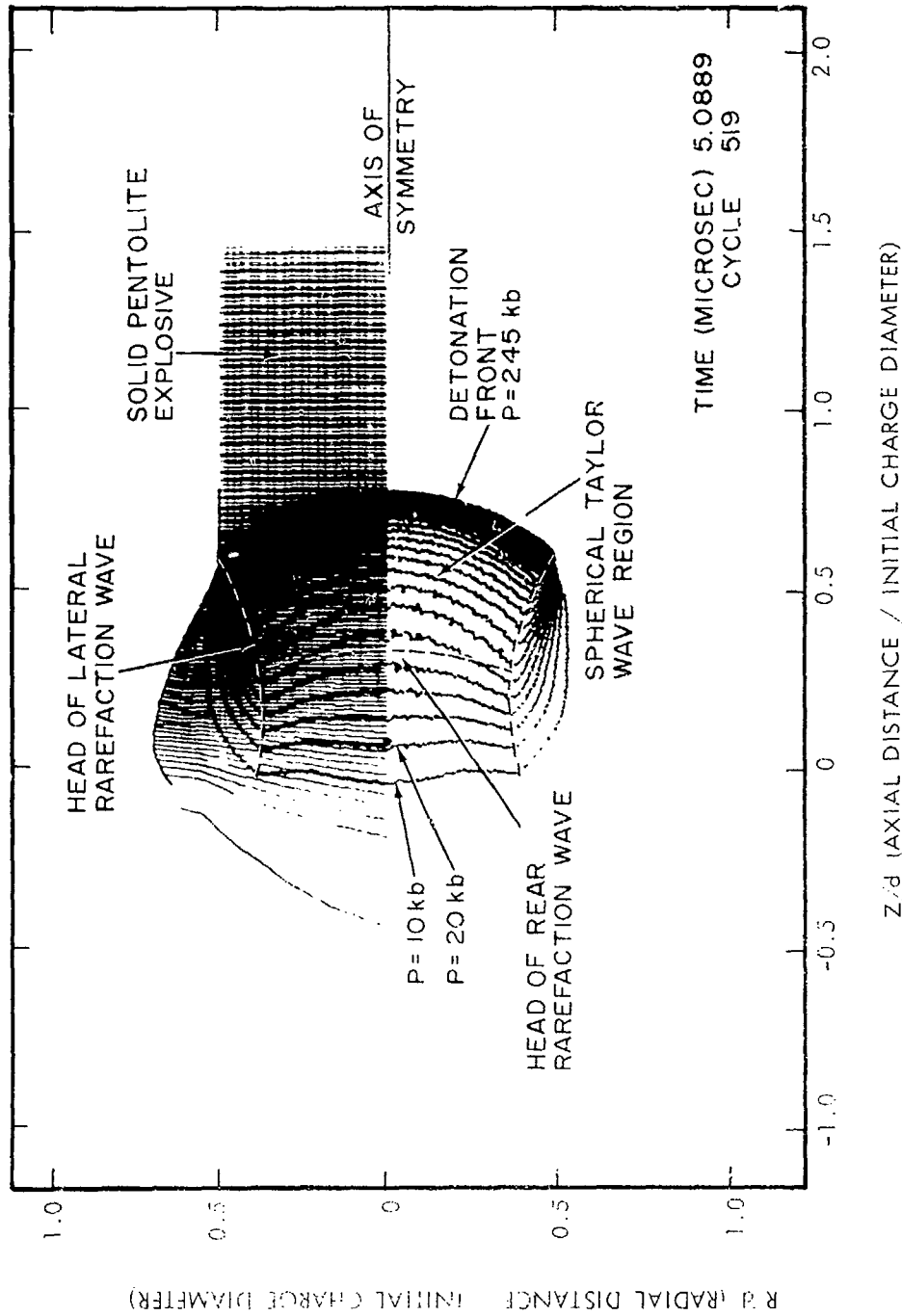
FIG. 8 The pressure distribution in the form of isobars is shown in the cross section of the detonating cylinder at 5.0889 μ seconds after initiation. There is a difference of 10kb between adjacent isobar lines. Point of initiation is at $(R/d, Z/d) = (0, 0)$.
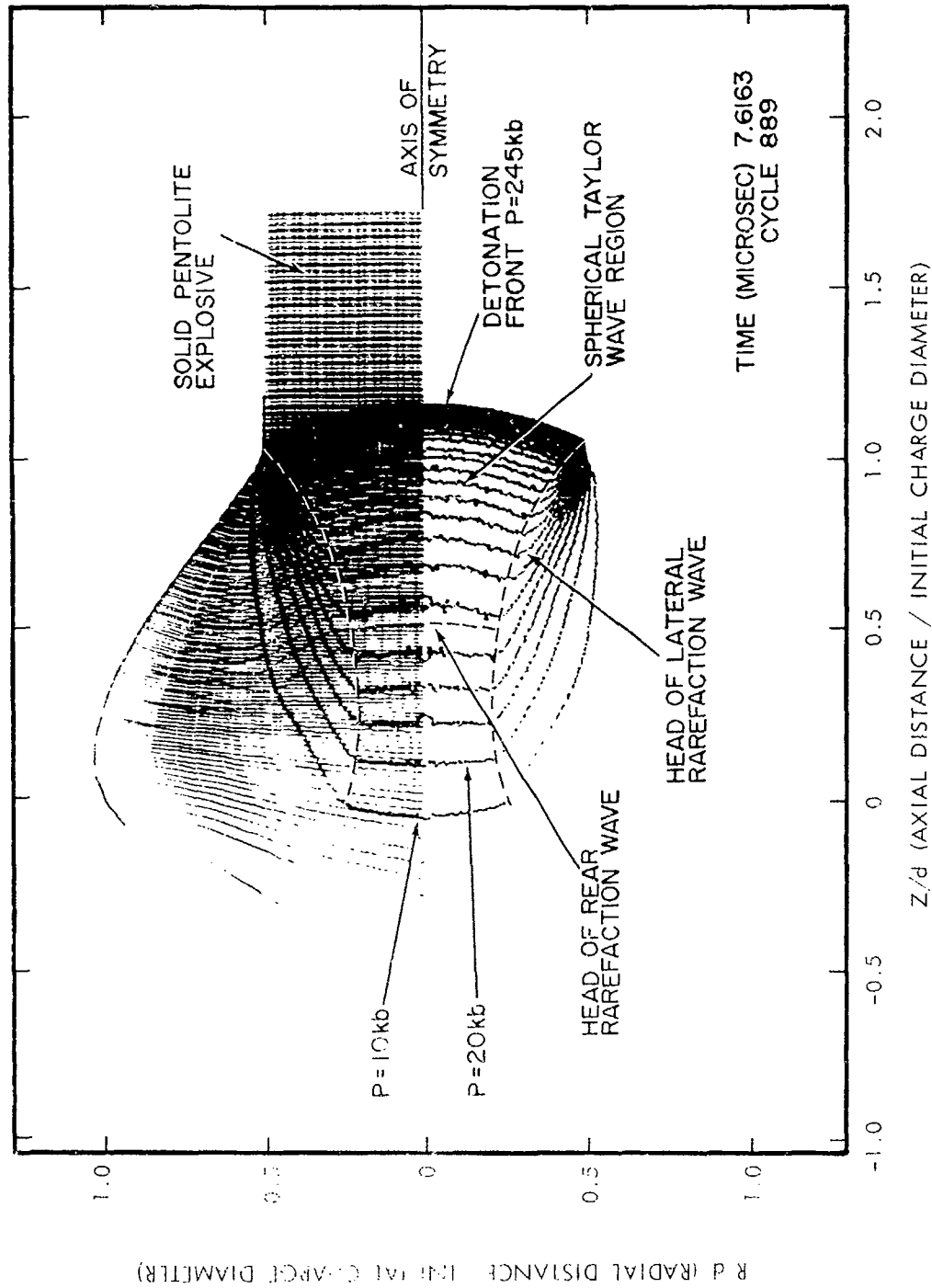
FIG. 9 The pressure distribution in the form of isobars is shown in the cross section of the detonating cylinder at 7.6163 μ seconds after initiation. There is a difference of 10kb between adjacent isobar lines. Point of initiation is at $(R/d, Z/d) = (0,0)$.
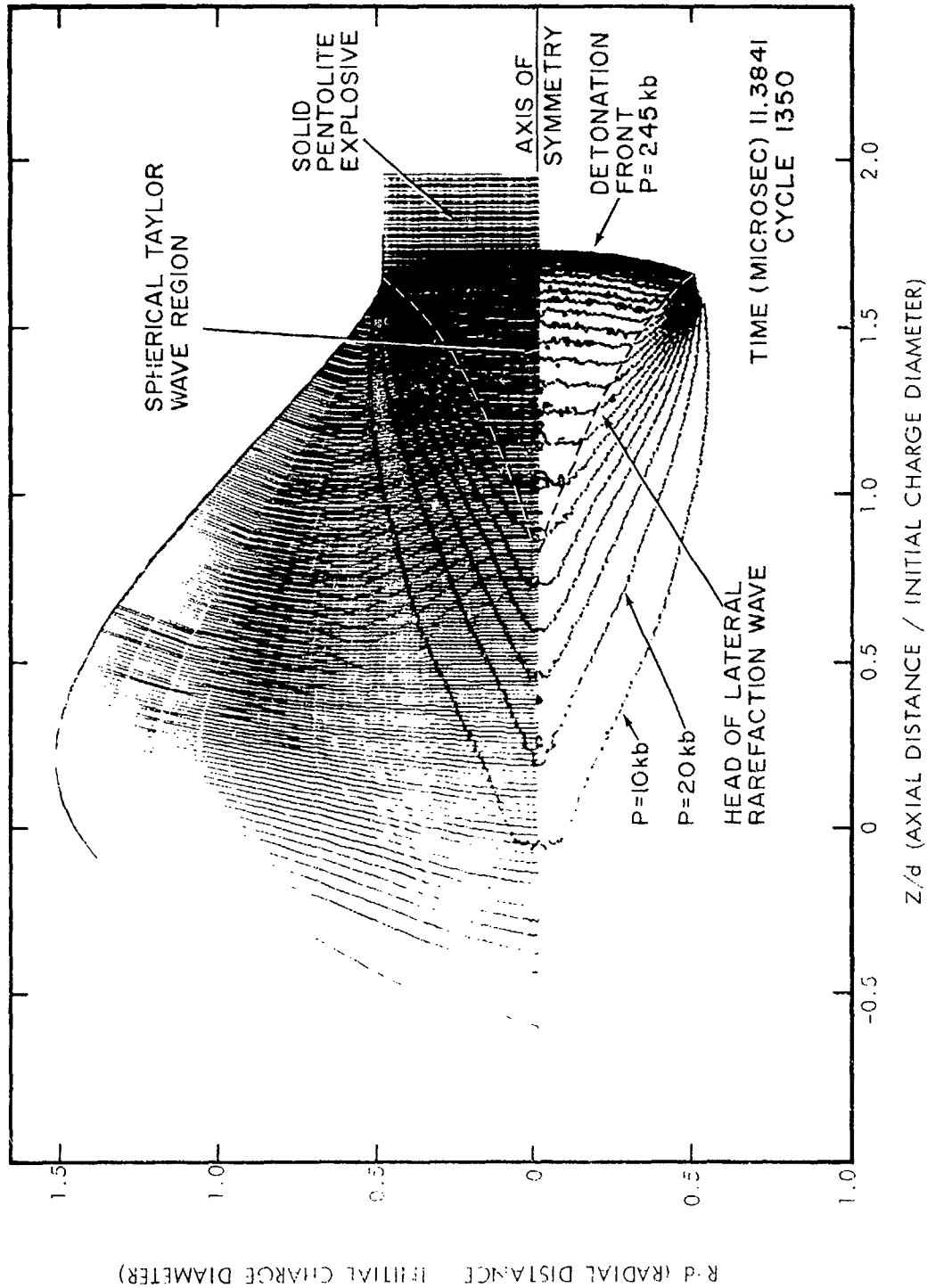
FIG. 10 The pressure distribution in the form of isobars is shown in the cross section of the detonating cylinder at 11.3841 μ seconds after initiation. There is a difference of 10kb between adjacent isobar lines. Point of initiation is at $(R/d, Z/d) = (0,0)$.
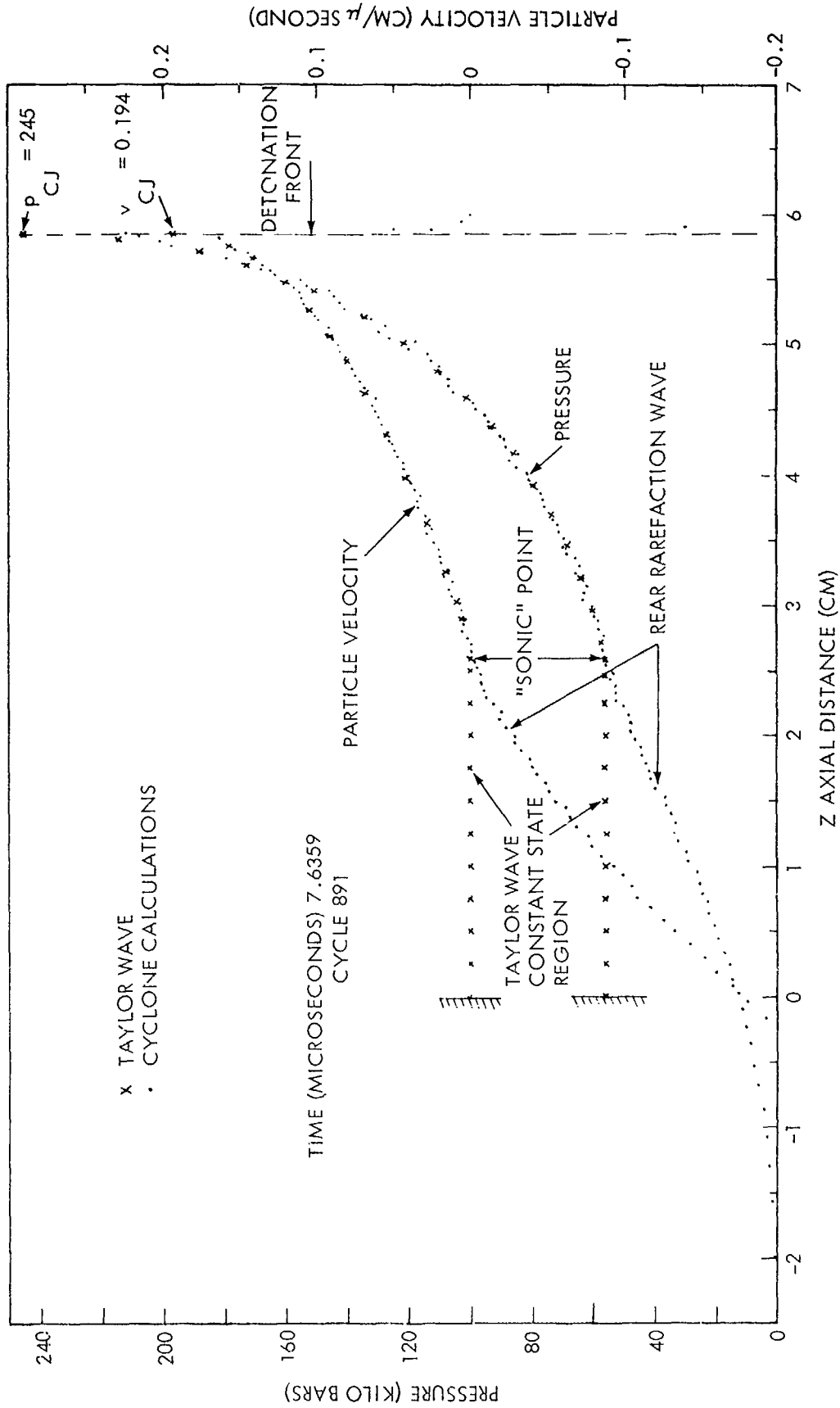
FIG. 11 Comparison of the pressure and particle velocity along the central axis (CYCLONE calculations) and the radial pressure and particle velocity distribution in a spherical Taylor wave. The CYCLONE values are taken at t=7.6359 microseconds after initiation. The Taylor wave was generated with the computer routines which are described in reference (13). Point of initiation is at Z=0.
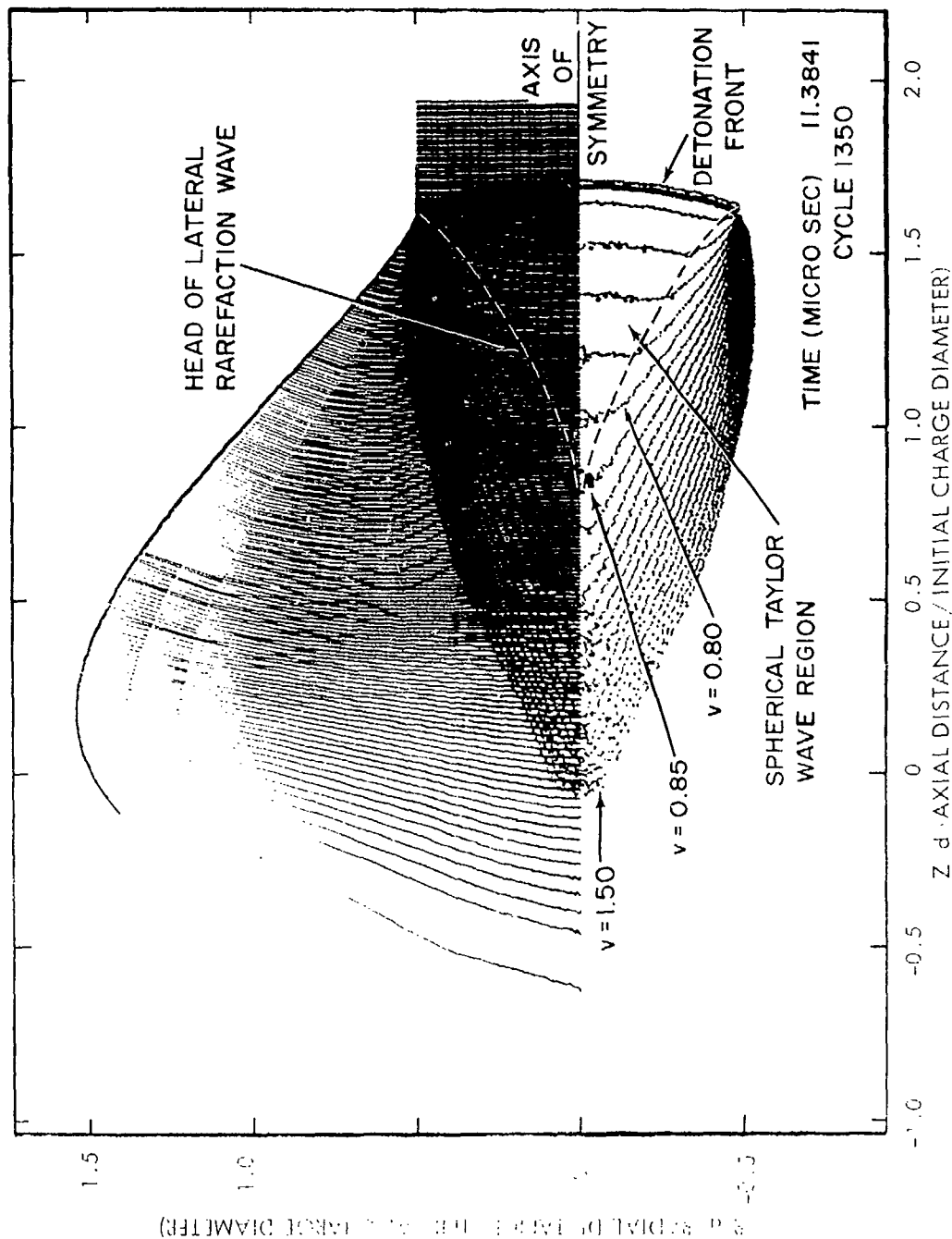
FIG. 12 The specific volume distribution in the cross section of the detonating cylinder at t = 11.3841 μ seconds. The isochore furthest from the detonation front is V = 1.50 cm³/g. The difference between isochores is 0.05 cm³/g. At the detonation front, V = 0.452 cm³/g. This isochore does not appear in the figure. The three lines at the detonation front (starting from the right V = 0.60, 0.55, and 0.50) are a result of the finite difference method which produces a continuous transition of the flow variables across the shock.

DISTRIBUTION

Copies

Technical Library
U. S. Naval Ordnance Station
Indian Head, Maryland 20640   1

Commanding Officer
Naval Weapons Station (ORR)
Yorktown, Virginia 23491   1

Commanding Officer & Director
David Taylor Model Basin
Washington, D. C. 20007
  Attn: Central Library Branch,
         Code 042-043   1

Commander
U. S. Naval Weapons Laboratory
Dahlgren, Virginia 22448
  Technical Library   1
    J. Talley   1
    D. Abernathy   1
  Terminal Ballistics Laboratory   1

Underwater Explosions Research Division
David Taylor Model Basin
Portsmouth, Virginia 23709   1

Commanding Officer
U. S. Army Ballistic Research
  Laboratories
Aberdeen Proving Ground, Md. 21005
  Attn: AMXBR-XS   1
         Dr. R. Eichelberger   1

Director
Applied Physics Laboratory
Johns Hopkins University
8621 Georgia Avenue
Silver Spring, Maryland 20910
  Attn: Document Librarian   1
         L. Welanetz   1
         M. Friedman   1

R. Stresau Laboratory, Inc.
Star Route
Spooner, Wisconsin 54801   1

APGC (PGBPS-12)
Eglin AFB, Florida 32542
  Attn: Virginia B. Harvey   1

Copies

Commander
Naval Air Systems Command
Washington, D. C. 20360
    AIR-604   1

Commanding General
Frankford Arsenal
Philadelphia, Pennsylvania 19137
    Attn: C2500, Library   1

Research Director, Explosives
    Research Center
Bureau of Mines
4800 Forbes Avenue
Pittsburgh, Pa., 15213
    Attn: R. W. Van Dolah   1

Systems Engr. Group (R&T)
Wright Patterson AFB, Ohio 45433
    SEPIR   1

Sandia Corporation
P. O. Box 969
Livermore, California 94550
    Attn: Document Control   1

Commanding General
U. S. Army Missile Command
Redstone Arsenal, Alabama 35809
    Attn: Technical Library   1

Sandia Corporation
P. O. Box 5800
Albuquerque, New Mexico 87115
    Attn: Technical Library   1

Commanding Officer
U. S. Naval Ordnance Laboratory
Corona, California 91720
    Library Division   1

Commanding Officer
Naval Underwater Weapons Research
    and Engineering Station
Newport, Rhode Island 02840   1

Commanding Officer
U. S. Naval Ammunition Depot
Crane, Indiana 47522
    QEL   1

Copies

Commander
U. S. Naval Ordnance Test Station
China Lake, California 93555
    Technical Library (Code 753)   1
    Dr. C. D. Lind   1

Superintendent
Naval Post Graduate School
Monterey, California 93940
    Code 2124   1

Lockheed Missile & Space Corporation
(LMSC)
599 S. Mathilda
Dept. 27-11
Sunnyvale, California 94086   1

Stanford Research Institute
Polymer and Propulsion Sciences Div.
Menlo Park, California 94025   1

Commanding Officer
U. S. Naval Weapons Evaluation
    Facility
Kirtland Air Force Base
Albuquerque, New Mexico 87117   1

Commanding Officer
Harry Diamond Laboratories
Connecticut Ave., & Van Ness
    Streets, N. W.
Washington, D. C. 20438
    Library   1

Defense Documentation Center
Cameron Station
Alexandria, Virginia 22314   20

Space Ordnance Systems, Inc.
122 Penn Street
El Segundo, California 90246
    Dell Lytle   1

Director
Naval Research Laboratory
Washington, D. C. 20390
    Code 2027   1

NASA Scientific and Technical
    Information Facility
P. O. Box 33
College Park, Maryland 20740   1

Copies

Commanding Officer
Picatinny Arsenal
Dover, New Jersey 07801
    SMUPA-G   1

	Copies
SMUPA-G	1
SMUPA-VA6	1
SMUPA-DD	1
SMUPA-DR4	1
SMUPA-DW	1
SMUPA-VC	1
SMUPA-VE	1
SMUPA-VL	1
SMUPA-TX	1
SMUPA-TW	1
SMUPA-W	1
SMUPA-DR	1

Army Materiel Command
Department of the Army
Washington, D. C. 20315
    R&D Division   1

NASA
Goddard Space Flight Center
Greenbelt, Maryland 20771   1

Director
Los Alamos Scientific Laboratory
P. O. Box 1663
Los Alamos, New Mexico 87544
    Attn: Report Librarian   1

Aerojet-General Corporation
Research Division
11711 Woodruff Avenue
Downey, California
    Attn: Dr. H. J. Fisher   1

Hercules Incorporated
Allegany Ballistics Laboratory
P. O. Box 210
Cumberland, Maryland 21502
    Attn: Technical Library   1

The Martin Company
Herndon Airport
815 Elwell Street
Orlando, Florida 32800
    J. Allred   1

Copies

Commanding General
Air Force Systems Command
Andrews Air Force Base
Camp Springs, Maryland 20331   1

The Boeing Company
Aero-Space Division
P. O. Box 3707
Scattle, Washington 98124
    Applied Math. Info. Center   1

New Mexico Institute of Mining & Technology
Campus Station
Socorro, New Mexico
    M. E. Hanson   1

Stanford University
Department of Aeronautical Engineering
Stanford, California 94305   1

The University of Texas
Defense Research Laboratory
P. O. Box 8029
Austin, Texas 78712   1

University of Washington
Department of Aeronautical Engineering
Seattle, Washington, 98122   1

Yale University
Department of Chemistry
New Haven, Connecticut
    Dr. John P. Chesick   1

Institute for Cooperative Research
Johns Hopkins University
1315 St. Paul Street
Baltimore, Maryland 21202   1

University of Missouri at Rolla
Rock Mechanics Research Group
Rolla, Missouri 65401
    Dr. R. Rollins   1

5

Copies

Shock Hydrodynamics, Inc.
Sherman Oaks, California 91403
    Dr. L. Zernow   1

Commander
Naval Air Development Center
Johnsville, Pennsylvania 18974
    Attn: Aviation Armament Laboratory   1

Commanding Officer
Office of Ordnance Research
Box CM
Duke Station
Durham, North Carolina 27706   1

Commanding Officer
Engineer Research & Development Laboratory
Ft. Belvoir, Virginia 22060
    Technical Intelligence Branch   1

Commanding Officer
U. S. Naval Weapons Evaluation Facility
Kirtland Air Force Base
Albuquerque, New Mexico 87117   1

Director
Lewis Research Center
National Aeronautics & Space Administration
21000 Brookpark Road
Cleveland, Ohio 44135   1

NASA
Langley Research Center
Hampton, Virginia 23365
    Attn: Mr. C. Breen   1

U. S. Atomic Energy Commission
Technical Information Extension
P. O. Box 62
Oak Ridge, Tennessee 37830   1

U. S. Atomic Energy Commission
Washington, D. C. 20545
    DMA   1

University of California
Lawrence Radiation Laboratory
Livermore, California 94550
    Attn: M. Wilkins   1

Copies

Aeronautical Engineering Review
2 East 64th Street
New York, New York 14304   1

Mechanics Research Department
American Machine and Foundry Co.
188 W. Randolph Street
Chicago, Illinois 60601   1

ITT Research Institute
10 West 35th Street
Chicago, Illinois 66616
        Attn: J. Kennedy   1

Atlantic Research Corporation
Alexandria, Virginia 22304
        Attn: Dr. A. Macek   1

AVCO-Everett Research Laboratory
2385 Revere Beach Parkway
Everett, Massachusetts 02149   1

AVCO-Manufacturing Company
155 Sniffins Lane
Stratford, Connecticut 06947   1

AVCO-Manufacturing Company
Research & Advanced Development Division
20 South Union Street
Lawrence, Massachusetts 01843
        Chief, Technical Library   1

AVCO Research Laboratory
2385 Revere Beach Parkway
Everett, Massachusetts 02149   1

Bell Aircraft Corporation
P. O. Box 1
Buffalo, New York 14201
        Attn: Library   1

Boeing Airplane Company
Box 3107
Seattle, Washington 98114   1

CONVAIR
P. O. Box 1011
Pomona, California 91769
        Attn: Library   1

Copies

Douglas Aircraft Company, Inc;
827 Lapham Street
El Segundo, California 90245
    Attn: Library   1

Cornell Aeronautical Lab., Inc.
4455 Gennessee Street
Buffalo, New York 14225
    Attn: Library   1

Fairchild Engine and Aircraft Co.
Guided Missiles Division
Wyandanch, L. I., New York 11798
    Attn: Library   1

General Applied Science Lab., Inc.
Meadowbrook National Bank Building
60 Hempstead Avenue
Hempstead, New York 11552   1

General Electric Company
Aeroscience Laboratory - MSVD
3750 D Street
Philadelphia, Pennsylvania 19124
    Attn: Dr. H. Lew   1

General Electric Company
Research Laboratory
P. O. Box 1088
Schenectady, New York 12301
    Attn:' Clarence Vogler   1

Grumman Aircraft Engineering Corporation
Bethpage, L. I., New York 11714
    Attn: Library   1

Hughs Aircraft Company
Research and Development Laboratories
Culver City, California 90230
    Attn: Library   1

North American Aviation, Inc.
Aerophysics Department
12214 Lakewood Blvd.
Downey, California 90241   1

Plasmadyne
3839 S. Main Street
Santa Ana, California 92707
    Attn: Dr. R. Waniek   1

Copies

Radio Corporation of America
Princeton, New Jersey 08540

1

Rand Corporation
1700 Main Street
Santa Monica, California 90401

1

RIAS, Inc.
7212 Bellona Avenue
Baltimore, Maryland 21212
    Attn: Library

1

Rocketdyne
Canoga Park, California 91303

1

Rohm and Haas Company
Redstone Arsenal Research Division
Huntsville, Alabama 35801

1

United Aircraft Corporation
Research Department
400 Main Street
East Hartford, Connecticut 06118
    Attn: Library

1

Vitro Laboratories
East Orange, New Jersey 07019

1

Vitro Laboratories
West Orange Laboratory
200 Pleasant Valley Way
West Orange, New Jersey 07052

1

Brown University
Division of Engineering
Providence, Rhode Island 02912
    Attn: Library

1

University of California
Engineering Department
Los Angeles, California 90024

1

California Institute of Technology
Guggenheim Aeronautical Laboratory
Pasadena, California 91109

1

California Institute of Technology
Jet Propulsion Laboratory
4800 Oak Grove Drive
Pasadena, California 91107

1

Copies

Carnegie Institute of Technology
Shenley Park
Pittsburgh, Pennsylvania 15213
  Attn: Dr. E. M. Pugh   1

Catholic University of America
Aeronautical Mechanical Engineering
Washington, D. C. 20017
  Attn: Library   1

Institute for Air Weapons Research
University of Chicago
Chicago, Illinois 60637   1

Denver Research Institute
University of Denver
Denver, Colorado 30210   1

Department of Civil Engineering
  and Engineering Mechanics
Columbia University
New York, New York 10027   1

Cornell University
Graduate School of Aeronautical Engineering
Ithaca, New York 14850   1

College of Engineering
Drexel Institute of Technology
Philadelphia, Pennsylvania 19104   1

University of Florida
Engineering Mechanics Department
Gainesville, Florida 32601
  Attn: Library   1

Georgia Institute of Technology
Department of Mechanical Engineering
Atlanta, Georgia 30332
  Attn: Library   1

Harvard University
Cambridge, Massachusetts 02138
  Department of Engineering Sciences   1
  Department of Applied Physics   1

University of Illinois
Urbana, Illinois 61801
  Dept. of Theoretical & Applied Mechanics   1

Copies

University of Maryland
College Park, Maryland 20742
    Inst. for Fluid Dyn. and Applied Math   1
    Engineering Library   1

Massachusetts Institute of Technology
Fluid Dynamics Research Group
Cambridge, Massachusetts 02139   1

Naval Supersonic Laboratory
Massachusetts Institute of Technology
Cambridge, Massachusetts 02139   1

University of Minnesota
Rosemount Research Center
Rosemount, Minnesota 55068   1

University of North Carolina
Physics Department
Chapel Hill, North Carolina 27514   1

North Carolina State College
Division of Engineering Research
Raleigh, North Carolina 27067
    Technical Library   1

Ohio State University
Columbus, Ohio 43210
    Attn: Library   1

Aerodynamics Laboratory
Polytechnic Institute of Brooklyn
527 Atlantic Avenue
Freeport, New York 11520   1

Rensselaer Polytechnic Institute
Department of Aero. Engineering
Troy, New York 12180
    Attn: Library   1

University of Southern California
Engineering Center
3518 University Avenue
Los Angeles, California 90007   1

Director
U. S. Army Research & Development Laboratory
Ft. Belvoir, Virginia 22060
    Chief, Tech. Support Branch   1

Copies

Director
USAF Project Rand
VIA. U.S. Air Force Liaison Office
The Rand Corporation
1700 Main Street
Santa Monica, California 90400   1

U. S. Documents Officer
Office of the U. S. National
  Military Representative, SHAPE
APO 55
New York, New York 10000   1

Director
Defense Atomic Support Agency
Washington, D. C. 20301
       J. Moulton   1

U. S. Research Services
1811 Trousdale Drive
Burlingame, California 94010   1

President
Kaman Nuclear
Colorado Springs, Colorado 80900
      Attn: Dr. F. Shelton   1

Institute for the Study of Rate Processes
University of Utah
Salt Lake City, Utah 84112
      Attn: Dr. M. A. Cook   1

Director
Physics International Co.
2229 4th Street
Berkeley, California 94700
      Attn: Dr. C. Godfrey   1

Science Communication, Inc.
1079 Wisconsin Avenue, N. W.
Washington, D. C. 20007
      Attn: Mr. D. O. Myatt   1

Astrophysics Research Corporation
10889 Wilshire Blvd.
Los Angeles, California 94700
      Attn: Dr. A. Reifman   1

Copies

Philco Corporation
Aeronutronic Division & Philco Research
Ford Road
Newport Beach, California 92660   1

Houston Research Institute, Inc.
5417 Crawford Street
Houston, Texas 77004
   Mr. Clark Goodman   1

Forrestal Research Center Library
Aeronautical Sciences Bldg.
Princeton University
Princeton, New Jersey 08540
   Librarian   1

Space Sciences Laboratory
General Electric Company
P. O. Box 8555
Philadelphia, Pennsylvania 19101
   Dr. S. M. Scala   1

Falcon Research and Development
1441 Ogden Street
Denver, Colorado 80218
  Mr. Daniel K. Parks   1
  Mr. C. E. Eppinger   1

United Electrodynamics
P. O. Box 1650
Pasadena, California
  Mr. O. K. Kowallis   1

Southwest Research Institute
8500 Culebra Road
San Antonio, Texas 78206
   Dr. W. H. Chu   1

Office of Chief of Naval Operations
Operations Evaluation Group
Washington, D. C. 20350   1

NASA Scientific & Technical
  Information Facility
P. O. Box 5700
Bethesda, Maryland 20546   1

DOCUMENT CONTROL DATA - R & D

Security classification of title, body of abstract and indexing annotation must be entered when the overall report is classified)

1. ORIGINATING ACTIVITY *(Corporate author)*	2a. REPORT SECURITY CLASSIFICATION
U. S. Naval Ordnance White Oak, Silver Spring, Maryland	**UNCLASSIFIED**
	2b. GROUP

3. REPORT TITLE

NUMERICAL HYDRODYNAMIC CALCULATIONS OF THE FLOW OF THE DETONATION PRODUCTS FROM A POINT-INITIATED EXPLOSIVE CYLINDER

4. DESCRIPTIVE NOTES *(Type of report and inclusive dates)*

5. AUTHOR(S) *(First name, middle initial, last name)*

DANTE PIACESI, Jr.

6. REPORT DATE	7a. TOTAL NO. OF PAGES	7b. NO. OF REFS
13 January 1967	27	13

8a. CONTRACT OR GRANT NO.	9a. ORIGINATOR'S REPORT NUMBER(S)
b. PROJECT NO. ORD-033-221/092-1/F008-08-11 P.A.004	NOLTR 66-150
c.	9b. OTHER REPORT NO(S) *(Any other numbers that may be assigned this report)*
d.	

10. DISTRIBUTION STATEMENT

This document is subject to special export controls and each transmittal to foreign governments may be made only with prior approval of NOL.

11. SUPPLEMENTARY NOTES	12. SPONSORING MILITARY ACTIVITY
	Naval Ordnance Systems Command

13. ABSTRACT

With the use of the NOL two-dimensional hydrodynamics computer program (CYCLONE), a detailed numerical analysis is made of the flow in the product gas of a detonating cylinder of pentolite (50/50 PETN/TNT) explosive. The explosive cylinder is initiated at a point on the central charge axis at one end-face.

DD FORM 1473 (PAGE 1)
1 NOV 65

S/N 0101-807-6801

14 KEY WORDS	LINK A		LINK P		LINK C	
	ROLE	WT	ROLE	WT	ROLE	WT
Explosive Hydrodynamics Cylinder Two-dimensional flow						

Naval Ordnance Laboratory, White Oak, Md.
(NOL technical report 66-150)
NUMERICAL HYDRODYNAMIC CALCULATIONS OF THE
FLOW OF THE DETONATION PRODUCTS FROM A POINT-
INITIATED EXPLOSIVE CYLINDER, by D. Piacesi,
jr. 13 Jan. 1967. 27p. charts, tables. NOSC
task ORD-033-221/092-1/F008-08-11.
UNCLASSIFIED

With the use of the NOL two-dimensional hy-
drodynamics computer program (Cyclone), a de-
tailed numerical analysis is made of the flow
in the product gas of a detonating cylinder
of pentolite (50/50 PETN/TNT) explosive. The
explosive cylinder is initiated at a point on
the central charge axis at one end-face.

1. Explosives -
   Hydrodynamics
2. Explosives -
   Detonation
I. Title
II. Piacesi,
   Dante, jr.
III. Project

Abstract card is
unclassified.

Naval Ordnance Laboratory, White Oak, Md.
(NOL technical report 66-150)
NUMERICAL HYDRODYNAMIC CALCULATIONS OF THE
FLOW OF THE DETONATION PRODUCTS FROM A POINT-
INITIATED EXPLOSIVE CYLINDER, by D. Piacesi,
jr. 13 Jan. 1967. 27p. charts, tables. NOSC
task ORD-033-221/092-1/F008-08-11.
UNCLASSIFIED

With the use of the NOL two-dimensional hy-
drodynamics computer program (Cyclone), a de-
tailed numerical analysis is made of the flow
in the product gas of a detonating cylinder
of pentolite (50/50 PETN/TNT) explosive. The
explosive cylinder is initiated at a point on
the central charge axis at one end-face.

1. Explosives -
   Hydrodynamics
2. Explosives -
   Detonation
I. Title
II. Piacesi,
   Dante, jr.
III. Project

Abstract card is
unclassified.

Naval Ordnance Laboratory, White Oak, Md.
(NOL technical report 66-150)
NUMERICAL HYDRODYNAMIC CALCULATIONS OF THE
FLOW OF THE DETONATION PRODUCTS FROM A POINT-
INITIATED EXPLOSIVE CYLINDER, by D. Piacesi,
jr. 13 Jan. 1967. 27p. charts, tables. NOSC
task ORD-033-221/092-1/F008-08-11.
UNCLASSIFIED

With the use of the NOL two-dimensional hy-
drodynamics computer program (Cyclone), a de-
tailed numerical analysis is made of the flow
in the product gas of a detonating cylinder
of pentolite (50/50 PETN/TNT) explosive. The
explosive cylinder is initiated at a point on
the central charge axis at one end-face.

1. Explosives -
   Hydrodynamics
2. Explosives -
   Detonation
I. Title
II. Piacesi,
   Dante, jr.
III. Project

Abstract card is
unclassified.

Naval Ordnance Laboratory, White Oak, Md.
(NOL technical report 66-150)
NUMERICAL HYDRODYNAMIC CALCULATIONS OF THE
FLOW OF THE DETONATION PRODUCTS FROM A POINT-
INITIATED EXPLOSIVE CYLINDER, by D. Piacesi,
jr. 13 Jan. 1967. 27p. charts, tables. NOSC
task ORD-033-221/092-1/F008-08-11.
UNCLASSIFIED

With the use of the NOL two-dimensional hy-
drodynamics computer program (Cyclone), a de-
tailed numerical analysis is made of the flow
in the product gas of a detonating cylinder
of pentolite (50/50 PETN/TNT) explosive. The
explosive cylinder is initiated at a point on
the central charge axis at one end-face.

1. Explosives -
   Hydrodynamics
2. Explosives -
   Detonation
I. Title
II. Piacesi,
   Dante, jr.
III. Project

Abstract card is
unclassified.